Journal of Integrative Neuroscience

J. Integr. Neurosci. **2026**; 25(11): 54986
https://doi.org/10.31083/JIN54986

Short Communication

HSV-1 Peptide Sharing With Drebrin and EGR1: Analysis of Sequence Context, Immune-Epitope Outcomes, and Structural Accessibility for Potential Cross-Reactivity in Alzheimer's Disease

Angela Stufano[1], Antje Vogelgesang[2], Domenico Plantone[3], Agnes Flöel[2,4], Guglielmo Lucchese[5,*]

[1]Department of Medical and Surgical Sciences, University of Foggia, 71122 Foggia, Italy
[2]Department of Neurology, University Medicine Greifswald, 17475 Greifswald, Germany
[3]Department of Medicine, University of Siena, 53100 Siena, Italy
[4]German Centre for Neurodegenerative Diseases (DZNE) Standort Greifswald, 17489 Greifswald, Germany
[5]Department of Experimental Medicine, University of Salento, 73100 Lecce, Italy
*Correspondence: guglielmo.lucchese@unisalento.it (Guglielmo Lucchese)
Academic Editor: Bettina Platt
Submitted: 17 June 2026 Revised: 16 September 2026 Accepted: 30 September 2026 Published: 13 November 2026

Abstract

Background: Alzheimer's disease (AD) is characterized by neuropathological hallmarks including amyloid plaques and neurofibrillary tangles and neuronal and synaptic loss. Loss of drebrin, a postsynaptic actin-binding protein is specifically associated with synaptic loss in AD. Epidemiological observations concerning herpes simplex virus type 1 (HSV-1) and AD are heterogeneous, and strong HSV-1-specific humoral immunity has also been associated with reduced progression from mild cognitive impairment to AD. **Methods:** We evaluated exact hexapeptide sharing between the HSV-1 reference proteome and human drebrin A or early growth response protein 1 (EGR1), while explicitly testing the effects of local sequence composition, database outcome structure, and predicted accessibility. Sequence enrichment was assessed using ordinary residue shuffling and an exact overlapping-tripeptide-preserving null model. Shared motifs were further evaluated in the Immune Epitope Database using positive and negative-only structures with exact-length and study adjustment, outcome-aware positional mapping, and AlphaFold-based structural-accessibility analysis. **Results:** Drebrin A shared eight distinct sixmers with HSV-1 (19 occurrence matches), whereas EGR1 shared five (11 occurrences). Under ordinary residue shuffling, drebrin showed enrichment of distinct motifs and occurrences; under the exact overlapping-tripeptide-preserving null, distinct-motif enrichment disappeared (p = 0.220), while the drebrin occurrence count persisted (p = 0.0215; Holm-adjusted p = 0.0430). EGR1 was non-significant under the constrained null. In the Immune Epitope Database, crude differences between positive and negative-only structures were largely explained by epitope length for B-cell assays, with exact-length-adjusted odds ratios of 0.93–0.94 for the drebrin, EGR1, and combined motif sets. Study- and length-adjusted motif analyses found no robust positive enrichment; the strongest reproducible result was depletion of SSSSSS among positive T-cell structures. Outcome-aware positional maps showed that positive epitopes frequently contained flanking sixmers with stronger positive representation than the shared sixmer itself. AlphaFold-based analysis supported solvent accessibility or disorder for several human motifs, with SESEVE confidently surface-exposed in drebrin; viral structural evidence remained incomplete. **Conclusions:** These findings establish exact sequence sharing and identify structurally plausible candidate regions for possible HSV-1-drebrin cross-reactivity, while indicating that sequence identity alone is insufficient to demonstrate motif immunogenicity or immune cross-recognition. Direct binding and cross-competition experiments are warranted.

Keywords: Alzheimer's disease; drebrin; EGR1; HSV-1; peptide sharing; molecular mimicry; IEDB; predicted structural accessibility

1. Introduction

Drebrin is an actin-binding protein enriched in dendritic spines and postsynaptic compartments. Its loss from hippocampal synapses is a consistent feature of Alzheimer's disease (AD), correlates with disease progression, and is linked to impaired spine maturation, synaptic plasticity, and cognition [1,2,3,4,5,6,7,8]. Early growth response protein 1 (EGR1) is a nuclear transcription factor that can downregulate drebrin expression; experimental inhibition of EGR1 has improved neuropathology and cognition in AD models [9,10]. These observations identify drebrin abundance as a potentially important point of convergence between synaptic degeneration and transcriptional regulation.

Herpes simplex virus type 1 (HSV-1) has repeatedly been investigated as a contributor to AD, through direct neuronal infection, reactivation, inflammatory responses, and interactions with amyloid biology [11,12,13,14]. The epidemiological literature remains heterogeneous, and a high-avidity HSV-1 antibody response has been associated with a lower risk of progression from amnestic mild cognitive impairment to AD [15]. One possible explanation is that the biological effect of antiviral immunity depends on

Copyright: © 2026 The Author(s). Published by IMR Press.
This is an open access article under the CC BY 4.0 license.

Publisher's Note: IMR Press stays neutral with regard to jurisdictional claims in published maps and institutional affiliations.

the precise immune specificities generated rather than on seropositivity alone.

Earlier proteome-wide and epitope-oriented studies provide a broader framework for interpreting short peptide identities. Comparative analyses have shown that peptide sharing between infectious agents and the human proteome can be extensive, including matches involving human proteins associated with neurological and neurodegenerative phenotypes, and that some of these overlaps occur within compositionally simple or repetitive sequences [16,17,18,19,20,21,22,23,24]. Conversely, studies of experimentally defined epitopes in influenza A, human immunodeficiency virus type 1 (HIV-1), and *Mycobacterium tuberculosis* have indicated that immune recognition is influenced by sequence context and by the degree of similarity to the host proteome, with relatively host-dissimilar peptide segments frequently characterizing recognized determinants [16,17,18,19,20,22,23]. Taken together, these observations support the use of short peptide identity as a hypothesis-generating approach to prioritize candidate sequences for immunological testing, while also indicating that sequence sharing per se is insufficient to infer pathogenic molecular mimicry or immune cross-reactivity [24,25].

A shared peptide may be relevant only if it is generated or exposed, presented or recognized in a compatible immune context, and capable of eliciting cross-recognition. Short, compositionally simple motifs are particularly prone to recurrence and therefore demand null models that preserve local sequence architecture [24]. We accordingly treat exact sixmer identity as a screening unit rather than as evidence of a complete B-cell or T-cell epitope.

Drebrin is nevertheless a biologically plausible autoimmune target. Anti-drebrin antibodies have been reported in patients with seizures and suspected autoimmune encephalitis, with biochemical, histological, knockout-tissue, and functional validation [26]. A subsequent case report described anti-drebrin reactivity in serum and cerebrospinal fluid in an adolescent with autoimmune encephalitis, although concomitant anti-mGluR2 positivity and the use of a commercial cell-based assay limit antigen-specific attribution [27]. These observations do not link anti-drebrin immunity to HSV-1, but they support the relevance of testing candidate shared sequences experimentally.

The present study therefore asked four restricted questions: (1) which exact sixmers are shared between HSV-1 and drebrin A or EGR1; (2) whether their recurrence exceeds null expectations after preserving local tripeptide architecture and comparison with large length-matched human-protein sets; (3) whether the motifs are preferentially represented among positive rather than negative-only IEDB (Immune Epitope Database) structures after accounting for epitope length and study; and (4) whether the human and viral occurrences occupy sequence contexts compatible with accessibility as linear-peptide candidates. The proposed EGR1-related protective pathway is considered a speculative biological possibility rather than a demonstrated mechanism.

2. Materials and Methods

2.1 Sequence Datasets and Exact Sixmer Identification

The human sequences were drebrin A (DBN1 isoform 3; UniProt accession Q16643-3; 695 amino acids) and canonical EGR1 (P18146; 543 amino acids). The sequences contained 690 and 538 overlapping sixmer windows, respectively, corresponding to 687 and 526 distinct sixmers. The HSV-1 reference proteome was UniProt proteome UP000009294, strain 17, downloaded on 29 July 2026 [28,29]; it comprised 73 proteins and 37,798 distinct sixmers. Each human sequence was fragmented with a one-residue sliding window, and exact matches were located in the HSV-1 proteome. Both the number of distinct shared sixmers and the total number of human-occurrence × viral-occurrence matches were recorded.

Sixmer-level compositional simplicity was flagged when at least one of the following criteria was met: Shannon entropy <1.5 bits, no more than two unique residues, or a homopolymeric run of at least four residues. This operational flag was used for annotation and interpretation; it was not treated as a binary proxy for antigenicity.

2.2 Composition-Aware Permutation Tests and Human-Protein Comparators

For each target, 10,000 ordinary residue shuffles preserved sequence length and total amino-acid counts. A stricter null generated 10,000 randomized sequences preserving the exact multiset of all overlapping tripeptides. Each tripeptide ABC was represented as a directed edge AB→BC, and randomized Eulerian trails reconstructed sequences with identical overlapping-tripeptide counts. This preserves local composition, residue clustering, and repeat architecture substantially more closely than an unconstrained shuffle. The master random seed was 12,345. Empirical p-values were calculated as $(r+1)/(n+1)$, where r is the number of permutations with a statistic at least as large as observed. Holm correction was applied across the two a priori targets separately for each null model and statistic.

As a separate comparator analysis, the same sequence-sharing workflow was applied to reviewed human proteins in prespecified length ranges: 514 proteins of 674–716 amino acids for comparison with drebrin A and 549 proteins of 530–556 amino acids for comparison with EGR1 after exclusion of EGR1 itself. Target percentiles and the numbers of comparator proteins with equal or larger distinct-motif and occurrence counts were reported. Composition-preserving permutation results for the comparator proteins were corrected by Holm and Benjamini-Hochberg procedures. Holm correction was applied across the two a priori targets within each null-model; corrections were performed

separately for each null model and statistic and were not pooled across all permutation comparisons.

2.3 IEDB Outcome and Motif-Level Analyses

IEDB data were retrieved through the IEDB Query Application Programming Interface (API) on 5 August 2026 [30]. Queries used the API base https://query-api.iedb.org, with the bcell_search endpoint for B-cell assays and the tcell_search endpoint for T-cell assays; bcell_id and tcell_id, respectively, were used as assay identifiers. Human-host records were selected using the IEDB organism-Internationalized Resource Identifier (IRI) field for NCBI Taxonomy 9606. To accommodate the query syntax accepted by the API, the supplied code tests the selectors host_organism_iri_search=ov.{NCBITaxon:9606}, host_organism_iri=eq.NCBITaxon:9606, and host_organism_iri=cs.{NCBITaxon:9606} in this order and uses the first accepted form. For construction of the primary outcome universe, the requested fields were assay Identifier (ID), structure_id, linear_sequence, and qualitative_measure. Records were retrieved in pages of 10,000, ordered by ascending assay ID and paginated using the limit and offset parameters. Requests used up to four attempts with a 1-s initial backoff and a 0.10-s delay between pages.

B-cell and T-cell records were processed separately. Sequences were converted to uppercase and whitespace was removed; only linear amino-acid sequences of length ≥6 with a usable assay ID and structure_id were retained. Qualitative outcomes beginning with "Positive" or "Negative" (case-insensitive) were classified accordingly, whereas other outcome categories were excluded. For the primary analysis, records were deduplicated at the structure_id level within each assay category. Assay IDs associated with each structure were stored as unique sets, preventing repeated records for the same assay from being counted more than once. If the same structure_id was associated with conflicting linear sequences, that structure was excluded. A structure was classified as positive when at least one positive assay was present and as negative-only when one or more negative assays were present in the absence of any positive assay. Thus, negative assay records from mixed positive/negative structures were excluded from the negative-only group. Unique epitope structures were the primary analysis unit; assay-record analyses were retained as a sensitivity analysis, with positive records from mixed structures retained and their negative records omitted.

The primary set-level effect was the prevalence of at least one target motif among all positive structures relative to its prevalence among all negative-only structures. Because the probability of containing a sixmer increases with peptide length, odds ratios were adjusted for exact epitope length using Mantel-Haenszel stratification. Analyses were performed separately for drebrin, EGR1, and their union and were repeated after exclusion of SSSSSS.

For individual-motif analyses, a second study-aware extraction used the same API endpoints, human-host restriction, pagination, and outcome criteria but additionally retrieved reference_id, pubmed_id, assay_description, and source_organism_name. Records were deduplicated within each combination of assay category, IEDB reference, and structure_id; assay IDs were again stored as unique sets, and conflicting sequences for the same reference-structure combination were excluded. Records lacking a reference identifier were retained in a separate MISSING_REFERENCE stratum. Within each reference, a structure with any positive assay was classified as positive; otherwise, a structure with one or more negative assays was classified as negative-only.

Each individual motif was analysed using Cochran-Mantel-Haenszel stratification jointly by IEDB reference and exact epitope length. Sensitivity analyses additionally stratified by normalized assay-method category or source-organism group. Holm correction was applied within assay and adjustment families across individual motifs. Asymptotic results from one-event zero-cell strata were not interpreted as significant; for SPPRTP, the conditional probability of the single motif-containing structure being positive within its reference-length stratum was calculated exactly. The resulting complete structure-level universe contained 195,920 positive and 583,198 negative-only B-cell structures and 57,307 positive and 121,052 negative-only T-cell structures. "Negative-only" therefore denotes absence of a positive result among the curated IEDB assays represented in the retrieved dataset and should not be interpreted as universal evidence that a peptide is non-immunogenic.

This is supported directly by the scripts: the primary script implements API paging and the selected query fields, while its structure-building code explicitly implements sequence filtering, deduplication, conflicting-sequence exclusion, and the positive/negative-only hierarchy. The study-adjusted script separately groups by reference and structure and applies the same positive-dominant classification.

2.4 Positional Mapping

For every positive and negative-only IEDB structure containing a shared motif, the complete peptide was decomposed into overlapping sixmers and aligned so that the shared motif began at relative position 0. For each relative position, separate maps displayed log10(positive structures+1), log10(negative-only structures+1), and the log2 ratio of positive to negative-only prevalence using the complete assay-specific denominators. These maps were interpreted descriptively to determine whether the shared motif at position 0 or surrounding sequence showed the stronger positive/negative profile. Missing sequence windows were distinguished conceptually from ratios near zero.

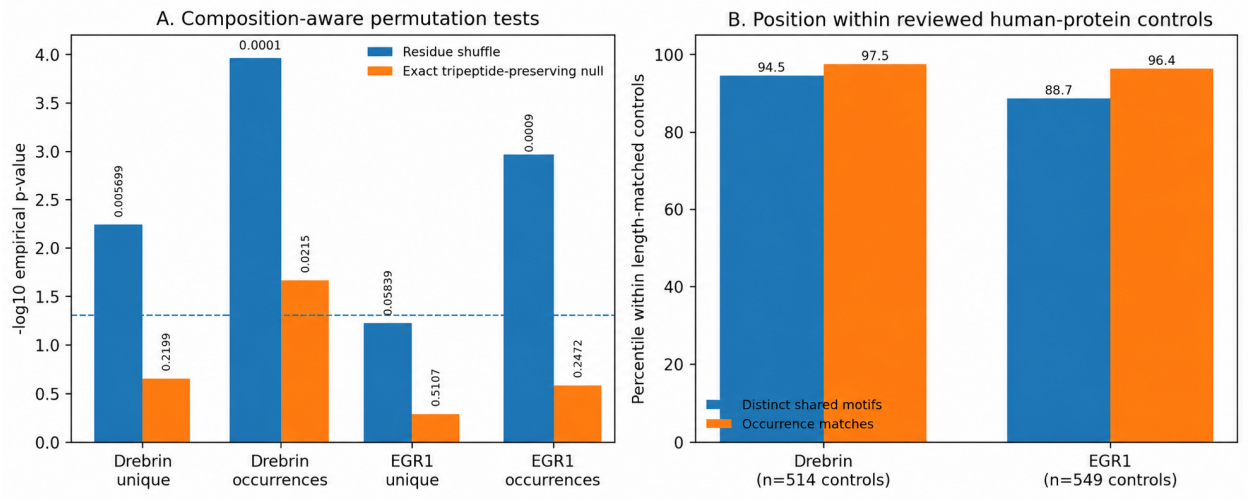


Fig. 1. Composition-aware sequence-sharing results. (A) Empirical *p*-values for distinct shared motifs and occurrence matches under ordinary residue shuffling and exact overlapping-tripeptide preservation. The dashed line indicates $p = 0.05$ before multiple-testing correction. (B) Target percentiles in reviewed length-matched human-protein comparator sets. These percentiles describe upper-tail position, not target specificity.

2.5 Structural-Accessibility Analysis

All human and viral occurrences were located in their full-length sequences. Human AlphaFold Database models were analysed when an exact sequence mapping was available [31]. Solvent-accessible surface area was estimated using a focused Shrake-Rupley approximation with a 1.4 Å probe and 240 sphere points per atom. Relative solvent accessibility (RSA) ≥0.25 was classified as exposed, while mean motif pLDDT <50 indicated low-confidence or disordered geometry. UniProt sequence annotations were used to describe viral low-complexity, repetitive, or disordered regions [28]. AlphaFold-based structural analysis was therefore restricted to the human side of each shared motif. Comparable structural models were unavailable for the analysed HSV-1 accessions; consequently, human–viral structural equivalence, including similarity of solvent exposure or local conformation, could not be assessed.

All analyses were hypothesis-generating. Predicted accessibility, IEDB association, or exact sequence identity was not interpreted as direct evidence of antibody binding, antigen processing, MHC presentation, T-cell recognition, or human-viral cross-reactivity.

3. Results

3.1 Exact Sequence Sharing and Composition-Aware Null Models

Drebrin A shared eight distinct sixmers with HSV-1: AAPQTP, PEPPAT, PLPPPP, PPPPPA, PRAPTP, SESEVE, SPPRTP, and SSSSSS. Multiple occurrences of SSSSSS in both proteins produced 19 total occurrence matches, of which 12 involved SSSSSS. EGR1 shared five distinct sixmers: ASSSSA, SSASAS, SSGGGG, SSSSAP, and SSSSSS, producing 11 occurrence matches (Table 1).

Under ordinary residue shuffling, drebrin showed enrichment for distinct motifs ($p = 0.00570$; Holm $p = 0.0114$) and occurrences ($p = 0.000100$; Holm $p = 0.000200$). Under the exact tripeptide-preserving null, the distinct-motif result was not significant ($p = 0.2199$; Holm $p = 0.4398$), whereas the occurrence count retained a modest signal ($p = 0.0215$; Holm $p = 0.0430$). EGR1 was non-significant for distinct motifs under both the residue-shuffle ($p = 0.0584$; Holm $p = 0.0584$) and tripeptide-preserving null ($p = 0.5107$; Holm $p = 0.5107$). Its residue-shuffle occurrence result was significant ($p = 0.000900$; Holm $p = 0.000900$), but the signal disappeared under tripeptide preservation ($p = 0.2472$; Holm $p = 0.2472$) (Fig. 1A).

Within the reviewed length-matched comparator sets, drebrin was at the 94.5th percentile for distinct motifs and the 97.5th percentile for occurrences; 28/514 and 13/514 control proteins, respectively, had equal or greater counts. EGR1 was at the 88.7th and 96.4th percentiles; 62/549 and 20/549 controls had equal or greater counts. No target or comparator remained significant after Holm correction under the composition-preserving model (Fig. 1B).

3.2 Outcome-Aware IEDB Analyses

In the crude structure-level analysis, the combined motif sets appeared less frequent among positive than negative-only B-cell structures. This difference was almost completely removed after exact epitope-length adjustment. The Mantel-Haenszel odds ratios were 0.934 for drebrin motifs (95% CI 0.687–1.268; $p = 0.660$), 0.933 for EGR1 motifs (0.657–1.324; $p = 0.700$), and 0.944 for the union (0.710–1.254; $p = 0.693$). Exclusion of SSSSSS also produced null B-cell estimates (OR 0.954–1.070; all $p \geq 0.776$).

Table 1. Exact HSV-1-human sixmer matches, positions, composition flag, and human structural context.

Human target	Sixmer	Human position(s)	HSV-1 protein/ accession	Viral position(s)	Compositionally simple	Human structural context
Drebrin A	AAPQTP	601–606	TRM2/P10217	92–97	No	RSA 0.740; pLDDT 33.5; disordered/low confidence
Drebrin A	PEPPAT	583–588	ICP34.5/P36313	157–162	No	RSA 0.747; pLDDT 48.9; disordered/low confidence
Drebrin A	PLPPPP	412–417	UL12/P04294	50–55	Yes	RSA 0.742; pLDDT 68.4; exposed, geometry uncertain
Drebrin A	PPPPPA	415–420	ICP34.5/P36313	47–52	Yes	RSA 0.745; pLDDT 64.9; exposed, geometry uncertain
Drebrin A	PRAPTP	539–544	ICP22/P04485	158–163	No	RSA 0.740; pLDDT 40.3; disordered/low confidence
Drebrin A	SESEVE	272–277	ICP22/P04485	39–44	Yes*	RSA 0.490; pLDDT 82.9; exposed and supported
Drebrin A	SPPRTP	342–347	ICP4/P08392	106–111	No	RSA 0.717; pLDDT 36.8; disordered/low confidence
Drebrin A	SSSSSS	334–339; 335–340; 336–341; 337–342	ICP4/P08392	186–191; 193–198; 194–199	Yes	RSA 0.679–0.698; pLDDT 36.2–37.2; disordered
EGR1	ASSSSA	169–174	ICP0/P08393	559–564; 564–569	Yes	RSA 0.681; pLDDT 39.8; disordered
EGR1	SSASAS	180–185	ICP0/P08393	585–590	Yes	RSA 0.662; pLDDT 42.6; disordered
EGR1	SSGGGG	66–71	ICP0/P08393	303–308	Yes	RSA 0.755; pLDDT 39.1; disordered
EGR1	SSSSAP	170–175	ICP0/P08393	565–570	Yes	RSA 0.687; pLDDT 40.4; disordered
EGR1	SSSSSS	62–67; 79–84	ICP4/P08392	186–191; 193–198; 194–199	Yes	RSA 0.661–0.692; pLDDT 35.0–40.8; disordered

*SESEVE was flagged by the prespecified entropy threshold (<1.5 bits) despite having no long homopolymeric run. HSV-1 position annotations refer to the UniProt strain-17 reference proteome. Viral structure models were unavailable. HSV-1, herpes simplex virus type 1; RSA, relative solvent accessibility; EGR1, early growth response protein 1.

For T-cell structures, the all-motif sets were negatively associated with positive outcomes (Drebrin OR 0.339, p = 0.0256; EGR1 OR 0.221, p = 0.0068; union OR 0.398, p = 0.0285). This pattern disappeared after excluding SSSSSS: the corresponding odds ratios (ORs) were 1.271, 0.679, and 0.972 (all $p \geq 0.658$).

Study- and exact-length-adjusted individual-motif analyses identified no robust positive enrichment (Table 2). PRAPTP had four positive and two negative-only B-cell structures, but its adjusted OR was 1.60 (p = 0.668). PLPPPP had three positive and nine negative-only T-cell structures and an imprecise adjusted OR of 6.00 (p = 0.330). SPPRTP was present in one positive and no negative-only B-cell structure in a single unrelated study. The asymptotic zero-cell estimate was not interpreted; the exact conditional probability was p = 0.057 before correction and therefore does not constitute evidence of SPPRTP enrichment. The most stable motif-level result was depletion of SSSSSS among positive T-cell structures (2 positive, 37 negative-only; OR 0.075; p = 0.0069; Holm p = 0.0415), which persisted in leave-one-study-out analyses.

3.3 Positional Sequence Context

The revised positional maps separated positive and negative-only structures and normalized counts by the complete assay-specific denominators.

PRAPTP and SPPRTP showed visually positive B-cell profiles at position 0, while SSASAS showed the same pattern in the T-cell data. These patterns were sparse or unsupported by adjusted inference. In contrast, SSSSSS showed a consistently negative T-cell profile, concordant with its study-adjusted depletion.

Fig. 2 presents selected balance maps; complete positive-count, negative-only-count, and balance panels are provided in the **Supplementary Material**.

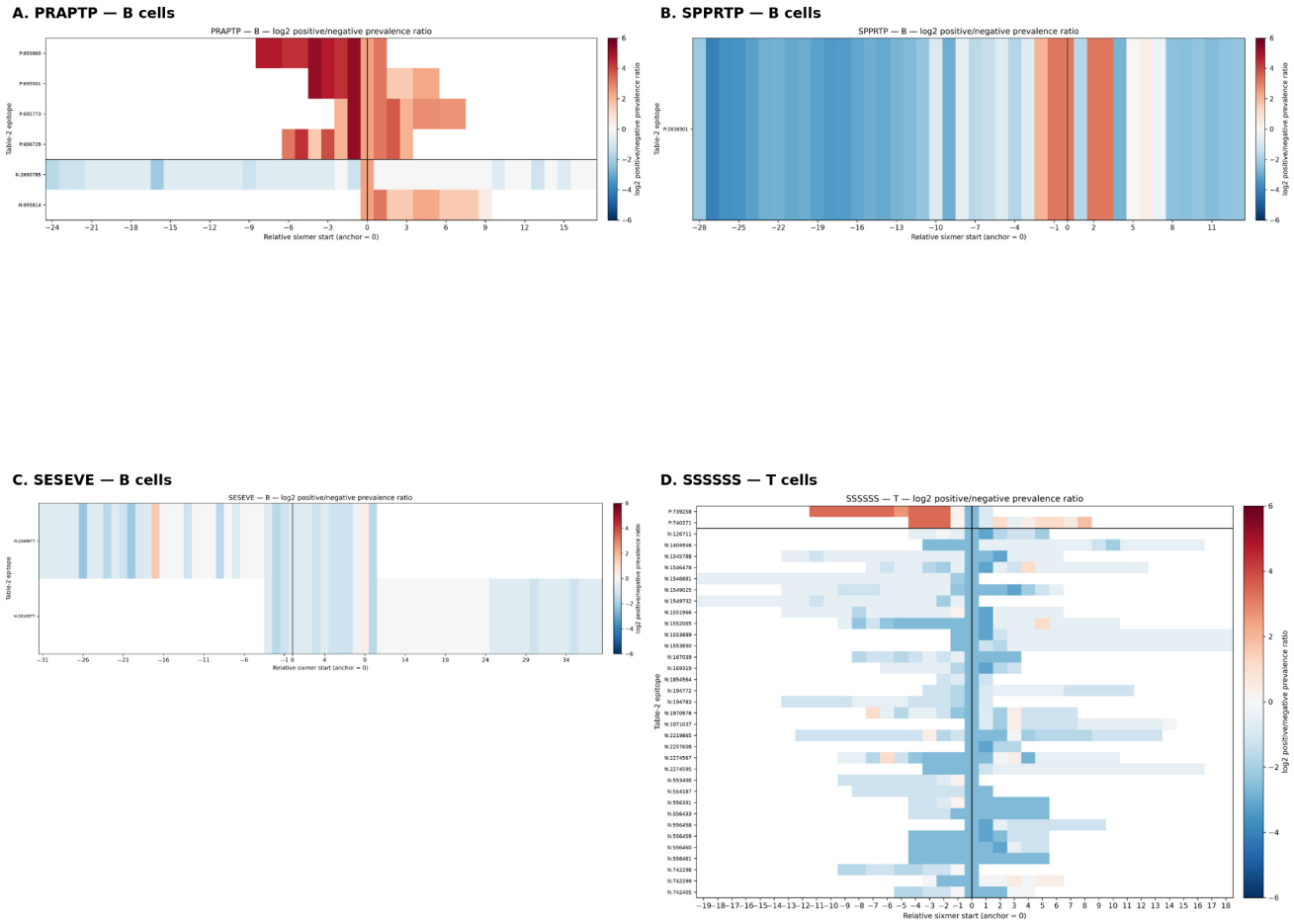


Fig. 2. Selected outcome-aware positional maps. Each map is centred on the shared motif (relative start 0) and displays the log2 ratio of positive to negative-only prevalence for overlapping sixmers across IEDB structures containing that motif. Red indicates greater positive representation and blue greater negative-only representation. (A) PRAPTP, B-cell assays: the shared motif lies within a locally positive profile, although the study- and length-adjusted motif association was not significant. (B) SPPRTP, B-cell assays: the anchor shows positive representation, but evidence was limited to a single positive structure and remained statistically inconclusive. (C) SESEVE, B-cell assays: the motif showed no positive IEDB support and was embedded predominantly in neutral-to-negative sequence context. (D) SSSSSS, T-cell assays: the shared motif and surrounding sequence showed a predominantly negative profile, consistent with the significant depletion of SSSSSS among positive T-cell structures. The maps are descriptive; isolated extreme cells can arise from small counts and should be interpreted together with the complete count panels in the supplement.

3.4 Structural and Biological Plausibility

All analysed human occurrences had high predicted solvent exposure. SESEVE was the only drebrin motif combining exposure with strong local AlphaFold confidence (mean RSA 0.490; mean pLDDT 82.9). PLPPPP and PPPPPA were highly exposed (mean RSA approximately 0.74) with intermediate pLDDT, supporting exposure but not a stable local geometry. The remaining drebrin motifs and all EGR1 motifs were exposed within low-confidence regions compatible with intrinsic disorder. Viral UniProt annotations placed most corresponding HSV-1 occurrences in disordered, repetitive, or compositionally biased regions, but quantitative viral RSA and pLDDT could not be calculated. Every human-viral pair therefore remained structurally incomplete.

The broad anti-drebrin antibody-reactive regions reported by Pitsch et al. [26] provide independent region-level plausibility. After alignment of the 649-amino-acid drebrin E2 construct used in that study with drebrin A, the PLPPPP/PPPPPA region corresponds to the antibody-reactive 319–444 fragment, and AAPQTP corresponds to the antibody-reactive 536–649 fragment. This does not identify those sixmers as the antibody-binding determinants, but it prioritizes their containing regions for direct peptide-level testing.

4. Discussion

The analyses identify drebrin as a prioritised candidate for experimental investigation of HSV-1–human cross-reactivity, without establishing immunological cross-

Table 2. Motif-level IEDB outcome evidence and human structural interpretation.

Sixmer	Target	B positive/ negative-only	Study+length-adjusted B	T positive/ negative-only	Study+length-adjusted T	Integrated interpretation
AAPQTP	Drebrin	0/0	Not estimable	0/0	Not estimable	Exposed but low-confidence; no IEDB evidence
PEPPAT	Drebrin	0/12	OR 0; $p = 0.624$	0/0	Not estimable	Exposed but low-confidence; no positive support
PLPPPP	Drebrin	5/48	OR 1.04; $p = 0.952$	3/9	OR 6.00; $p = 0.330$	Exposed; low-complexity; context-dependent
PPPPPA	Drebrin	12/158	OR 1.28; $p = 0.496$	1/7	OR 0.18; $p = 0.272$	Exposed; low-complexity; no robust enrichment
PRAPTP	Drebrin	4/2	OR 1.60; $p = 0.668$	0/1	OR 0; $p = 0.844$	Non-simple candidate; adjusted-null
SESEVE	Drebrin	0/2	OR 0; $p = 0.728$	0/0	Not estimable	Only confidently exposed Drebrin motif; no positive IEDB support
SPPRTP	Drebrin	1/0	Exact $p = 0.057$	0/0	Not estimable	Non-simple; one-study observation; hypothesis-generating
ASSSSA	EGR1	2/16	OR 2.07; $p = 0.321$	0/8	OR 0; $p = 0.780$	Disordered; low-complexity
SSASAS	EGR1	0/11	OR 0; $p = 0.415$	2/0	Not estimable	Sparse T-cell positivity; low-complexity
SSGGGG	EGR1	7/60	OR 0.75; $p = 0.692$	0/0	Not estimable	Disordered; low-complexity
SSSSAP	EGR1	1/13	OR 1.28; $p = 0.814$	0/1	OR 0; $p = 0.691$	Disordered; low-complexity
SSSSSS	Both	34/358	OR 1.12; $p = 0.624$	2/37	OR 0.075; Holm $p =$ 0.0415	Highly recurrent homopolymer; T-cell depletion

Counts are unique IEDB peptide structures. Mixed positive/negative structures were classified as positive within each assay category. ORs are Mantel-Haenszel estimates stratified by IEDB reference and exact peptide length. Sparse non-estimable cells are shown without asymptotic inference. OR, odds ratio; IEDB, Immune Epitope Database.

recognition. Exact sixmer sharing between HSV-1 and drebrin/EGR1 is reproducible, but the statistical meaning depends strongly on the null model. Drebrin remains in the upper tail of length-matched proteins and retains significant occurrence-level sharing with the virus under exact tripeptide preservation. EGR1 sharing appears to lose significance with more restrictive null hypotheses. These results justify drebrin as a candidate for HSV-1-specific cross-reaction.

The IEDB analyses further distinguish motif occurrence in experimentally tested peptides from motif-driven immunogenicity. Shared motifs were found in both positive and negative-only records. The crude B-cell deficit was caused largely by peptide-length imbalance, and adjusted set-level estimates were null. Individual study-adjusted analyses likewise found no robust positive motif enrichment. The outcome-aware positional maps showed why simple recurrence counts were misleading: several positive peptides contained more positively represented flanking sequences than the shared sixmer itself. The shared sixmers may therefore lie within immunoreactive peptides without constituting the minimal reactive determinant.

Despite these statistical limits, several observations support experimental plausibility. Drebrin is an independently reported human autoantigen [26,27]. Of note, the epitopic sequence experimentally identified as driving autoimmune recognition does indeed include the 6-mers PLPPPP and PPPPPA [26]. Other drebrin motifs are solvent exposed or located in disordered regions accessible as linear peptide segments. PRAPTP is a non-simple motif with the most favourable B-cell count balance among the better-populated motifs, although its ad-

justed estimate is null. SPPRTP is non-simple, exposed in a disordered drebrin A-specific segment, and had one positive IEDB observation, but the evidence is too sparse for enrichment. SESEVE has the strongest structural support but no positive IEDB record. No single motif therefore is entirely supported across sequence statistics, IEDB outcomes, structural confidence, and clinical region mapping. Of note, while naive sequence matching flags poly-serine repeats as major shared motifs, our outcome-aware positional mapping reveals a consistently negative T-cell profile for SSSSSS, effectively prioritizing non-simple candidate sequences for experimental validation.

The proposed EGR1 pathway requires particular caution. EGR1 is an intracellular nuclear protein, and recognition of an EGR1-derived peptide would not necessarily inhibit its transcriptional activity or selectively increase drebrin. T-cell recognition could instead damage antigen-expressing cells. Drebrin is also intracellular, although neuronal injury, antigen release, uptake, and processing could permit antibody or T-cell responses. The current data do not establish the effector arm, tissue access, antigen processing, or direction of biological effect. Consequently, EGR1 is retained only as a speculative counter-regulatory target that might be explored experimentally, not as an established explanation for protective HSV-1 immunity.

Limitations

Among the principal limitations of the present study, the use of IEDB negative-only outcomes is assay-context dependent, and study-level stratification cannot remove all differences in assay design, source organism, or publication practice. AlphaFold accessibility does not demonstrate exposure *in vivo* or binding by patient antibodies. Nevertheless, by combining composition-aware sequence analysis with length-matched human-protein comparisons and outcome-aware IEDB analyses that account for assay class, peptide length, study, and local sequence context, the revised workflow addresses the principal sources of bias identified in short-peptide sharing analyses.

Candidate autoantigen panels for unmasking anti-drebrin immunity should include the antibody-region motifs AAPQTP, PLPPPP, and PPPPPA; the non-simple PRAPTP and SPPRTP motifs; and structurally supported SESEVE, together with scrambled and composition-matched controls. For experimental follow-up, we prioritize AAPQTP, PLPPPP, and PPPPPA because they map to broad anti-drebrin antibody-reactive regions, with AAPQTP additionally avoiding the marked compositional simplicity of the proline-rich motifs. SESEVE, SPPRTP, and PRAPTP form a second tier: SESEVE has the strongest structural support, whereas SPPRTP and PRAPTP are compositionally non-simple but lack adjusted IEDB enrichment.

5. Conclusions

HSV-1 shares exact six-amino-acid sequences with drebrin A and EGR1. Composition-aware permutation tests, large length-matched human-protein controls, outcome-aware IEDB analyses, and structural mapping substantially narrow the interpretation of this sharing. The data support a set of accessible or disordered candidate peptide regions, particularly in drebrin and provide a prioritized, reproducible framework for direct experimental testing of HSV-1-drebrin cross-recognition with possible relevance to Alzheimer's disease.

Availability of Data and Materials

The complete analysis code used in this study is provided as **Supplementary Material**. Scripts are sufficient to reproduce the reported results, tables, and figures.

Author Contributions

AS: data curation, investigation, methodology, writing—original draft. AF and DP: validation, writing—review and editing. GL: conceptualization, data curation, investigation, methodology, project administration, writing—original draft, review and editing. AV: conceptualization, data curation, investigation, methodology, validation, writing—review and editing. All authors read and approved the final manuscript. All authors have participated sufficiently in the work and agreed to be accountable for all aspects of the work.

Ethics Approval and Consent to Participate

Not applicable.

Acknowledgment

Not applicable.

Funding

This research received no external funding.

Conflicts of Interest

The authors declare no conflicts of interest.

Supplementary Material

Supplementary material associated with this article can be found, in the online version, at https://doi.org/10.31083/JIN54986.

References

[1] Kojima N, Kato Y, Shirao T, Obata K. Nucleotide sequences of two embryonic drebrins, developmentally regulated brain proteins, and developmental change in their mRNAs. Brain Research. 1988; 464: 207–215. https://doi.org/10.1016/0169-328x(88)90027-7

[2] Aoki C, Sekino Y, Hanamura K, Fujisawa S, Mahadomrongkul V, Ren Y, et al. Drebrin A is a postsynaptic protein that localizes

in vivo to the submembranous surface of dendritic sites forming excitatory synapses. The Journal of Comparative Neurology. 2005; 483: 383–402. https://doi.org/10.1002/cne.20449

[3] Harigaya Y, Shoji M, Shirao T, Hirai S. Disappearance of actin-binding protein, drebrin, from hippocampal synapses in Alzheimer's disease. Journal of Neuroscience Research. 1996; 43: 87–92. https://doi.org/10.1002/jnr.490430111

[4] Ishizuka Y, Hanamura K. Drebrin in Alzheimer's Disease. Advances in Experimental Medicine and Biology. 2017; 1006: 203–223. https://doi.org/10.1007/978-4-431-56550-5_12

[5] Shim KS, Lubec G. Drebrin, a dendritic spine protein, is manifold decreased in brains of patients with Alzheimer's disease and Down syndrome. Neuroscience Letters. 2002; 324: 209–212. https://doi.org/10.1016/s0304-3940(02)00210-0

[6] Julien C, Tremblay C, Bendjelloul F, Phivilay A, Coulombe MA, Emond V, et al. Decreased drebrin mRNA expression in Alzheimer disease: correlation with tau pathology. Journal of Neuroscience Research. 2008; 86: 2292–2302. https://doi.org/10.1002/jnr.21667

[7] Liu Y, Xu Y, Zhang L, Huang L, Yu P, Zhu H, et al. Down-Regulated Drebrin Aggravates Cognitive Impairments in a Mouse Model of Alzheimer's Disease. International Journal of Molecular Sciences. 2017; 18: 800. https://doi.org/10.3390/ijms18040800

[8] Hatanpää K, Isaacs KR, Shirao T, Brady DR, Rapoport SI. Loss of proteins regulating synaptic plasticity in normal aging of the human brain and in Alzheimer disease. Journal of Neuropathology and Experimental Neurology. 1999; 58: 637–643. https://doi.org/10.1097/00005072-199906000-00008

[9] Cho C, MacDonald R, Shang J, Cho MJ, Chalifour LE, Paudel HK. Early growth response-1-mediated down-regulation of drebrin correlates with loss of dendritic spines. Journal of Neurochemistry. 2017; 142: 56–73. https://doi.org/10.1111/jnc.14031

[10] Qin X, Wang Y, Paudel HK. Inhibition of Early Growth Response 1 in the Hippocampus Alleviates Neuropathology and Improves Cognition in an Alzheimer Model with Plaques and Tangles. The American Journal of Pathology. 2017; 187: 1828–1847. https://doi.org/10.1016/j.ajpath.2017.04.018

[11] Catumbela CSG, Giridharan VV, Barichello T, Morales R. Clinical evidence of human pathogens implicated in Alzheimer's disease pathology and the therapeutic efficacy of antimicrobials: an overview. Translational Neurodegeneration. 2023; 12: 37. https://doi.org/10.1186/s40035-023-00369-7

[12] Bruno F, Abondio P, Bruno R, Ceraudo L, Paparazzo E, Citrigno L, et al. Alzheimer's disease as a viral disease: Revisiting the infectious hypothesis. Ageing Research Reviews. 2023; 91: 102068. https://doi.org/10.1016/j.arr.2023.102068

[13] Wozniak MA, Mee AP, Itzhaki RF. Herpes simplex virus type 1 DNA is located within Alzheimer's disease amyloid plaques. The Journal of Pathology. 2009; 217: 131–138. https://doi.org/10.1002/path.2449

[14] D'Aiuto L, Prasad KM, Upton CH, Viggiano L, Milosevic J, Raimondi G, et al. Persistent infection by HSV-1 is associated with changes in functional architecture of iPSC-derived neurons and brain activation patterns underlying working memory performance. Schizophrenia Bulletin. 2015; 41: 123–132. https://doi.org/10.1093/schbul/sbu032

[15] Agostini S, Mancuso R, Baglio F, Cabinio M, Hernis A, Costa AS, et al. High avidity HSV-1 antibodies correlate with absence of amnestic Mild Cognitive Impairment conversion to Alzheimer's disease. Brain, Behavior, and Immunity. 2016; 58: 254–260. https://doi.org/10.1016/j.bbi.2016.07.153

[16] Lucchese G, Capone G, Kanduc D. Peptide sharing between influenza A H1N1 hemagglutinin and human axon guidance proteins. Schizophrenia Bulletin. 2014; 40: 362–375. https://doi.org/10.1093/schbul/sbs197

[17] Kusalik A, Bickis M, Lewis C, Li Y, Lucchese G, Marincola FM, et al. Widespread and ample peptide overlapping between HCV and Homo sapiens proteomes. Peptides. 2007; 28: 1260–1267. https://doi.org/10.1016/j.peptides.2007.04.001

[18] Lucchese G, Stufano A, Kanduc D. Proteome-guided search for influenza A B-cell epitopes. FEMS Immunology and Medical Microbiology. 2009; 57: 88–92. https://doi.org/10.1111/j.1574-695X.2009.00582.x

[19] Kanduc D, Fanizzi FP, Lucchese G, Stevanovic S, Sinha AA, Mittelman A. NMR probing of in silico identification of anti-HPV16 E7 mAb linear peptide epitope. Peptides. 2004; 25: 243–250. https://doi.org/10.1016/j.peptides.2003.12.004

[20] Lucchese G, Stufano A, Calabro M, Kanduc D. Charting the peptide crossreactome between HIV-1 and the human proteome. Frontiers in Bioscience (Elite Edition). 2011; 3: 1385–1400. https://doi.org/10.2741/e341

[21] Trost B, Kusalik A, Lucchese G, Kanduc D. Bacterial peptides are intensively present throughout the human proteome. Self-/nonself. 2010; 1: 71–74. https://doi.org/10.4161/self.1.1.9588

[22] Kanduc D, Tessitore L, Lucchese G, Kusalik A, Farber E, Marincola FM. Sequence uniqueness and sequence variability as modulating factors of human anti-HCV humoral immune response. Cancer Immunology, Immunotherapy: CII. 2008; 57: 1215–1223. https://doi.org/10.1007/s00262-008-0456-y

[23] Lucchese G, Stufano A, Kanduc D. Proposing low-similarity peptide vaccines against Mycobacterium tuberculosis. Journal of Biomedicine & Biotechnology. 2010; 2010: 832341. https://doi.org/10.1155/2010/832341

[24] Maguire C, Wang C, Ramasamy A, Fonken C, Morse B, Lopez N, et al. Molecular mimicry as a mechanism of viral immune evasion and autoimmunity. Nature Communications. 2024; 15: 9403. https://doi.org/10.1038/s41467-024-53658-8

[25] Arévalo-Cortés A, Rodriguez-Pinto D, Aguilar-Ayala L. Evidence for Molecular Mimicry between SARS-CoV-2 and Human Antigens: Implications for Autoimmunity in COVID-19. Autoimmune Diseases. 2024; 2024: 8359683. https://doi.org/10.1155/2024/8359683

[26] Pitsch J, Kamalizade D, Braun A, Kuehn JC, Gulakova PE, Rüber T, et al. Drebrin Autoantibodies in Patients with Seizures and Suspected Encephalitis. Annals of Neurology. 2020; 87: 869–884. https://doi.org/10.1002/ana.25720

[27] Liu A, Huang J, Zhang J, Yan J. Adolescent autoimmune encephalitis with dual positive anti-Drebrin and anti-mGluR2 antibodies: a case report. Frontiers in Immunology. 2026; 17: 1711467. https://doi.org/10.3389/fimmu.2026.1711467

[28] UniProt Consortium. UniProt: the Universal Protein Knowledgebase in 2025. Nucleic Acids Research. 2025; 53: D609–D617. https://doi.org/10.1093/nar/gkae1010

[29] Ahmad S, Jose da Costa Gonzales L, Bowler-Barnett EH, Rice DL, Kim M, Wijerathne S, et al. The UniProt website API: facilitating programmatic access to protein knowledge. Nucleic Acids Research. 2025; 53: W547–W553. https://doi.org/10.1093/nar/gkaf394

[30] Vita R, Blazeska N, Marrama D, IEDB Curation Team Members, Duesing S, Bennett J, et al. The Immune Epitope Database (IEDB): 2024 update. Nucleic Acids Research. 2025; 53: D436–D443. https://doi.org/10.1093/nar/gkae1092

[31] Varadi M, Bertoni D, Magana P, Paramval U, Pidruchna I, Radhakrishnan M, et al. AlphaFold Protein Structure Database in 2024: providing structure coverage for over 214 million protein sequences. Nucleic Acids Research. 2024; 52: D368–D375. https://doi.org/10.1093/nar/gkad1011